# Metastability of two-dimensional vortex glass in $Bi_2Sr_2CaCu_2O_{8+\delta}$

A. Pallinger,[1] B. Sas,[1] G. Kriza,[1] K. Vad,[2] L. Forro,[3] H. Berger,[3] F. Portier,[4] and F. I. B. Williams[1,4]
[1]*Research Institute for Solid State Physics and Optics, P.O. Box 49, H-1525 Budapest, Hungary*
[2]*Institute for Nuclear Research, P.O. Box 51, H-4001 Debrecen, Hungary*
[3]*Institute of Physics of Complex Matter, Ecole Polytechnique Féderale de Lausanne, 1015 Lausanne, Switzerland*
[4]*Service de Physique de l'Etat Condensé, Direction des Sciences de la Matière, Commissariat à l'Energie Atomique, Saclay F-91191, Gif-sur-Yvette, France*
(Received 18 December 2008; revised manuscript received 1 June 2009; published 23 July 2009)

The decoupled layer quasi-two-dimensional glass phase of *c*-axis vortices in optimally doped $Bi_2Sr_2CaCu_2O_{8+\delta}$ (BSCCO) exhibits low-temperature metastability, the onset temperature of which is coincident with the peak in depinning current for zero-field-cooled sample preparation. We present experiments in strongly underdoped BSCCO showing similar metastability and develop a model for pinning dynamics where metastability results from progressive loss of thermal contact. The model accounts well for the field-temperature locus of the metastability and for the irreversibility and memory effects. We conclude that the metastability arises from a nonsingular dynamic crossover and does not mark a phase transition.

DOI: 10.1103/PhysRevB.80.024206 PACS number(s): 74.25.Qt, 71.55.Jv, 74.72.Hs

## I. INTRODUCTION

A two-dimensional (2D) glass differs from the usual three-dimensional (3D) structural glass. The latter is often viewed as a dynamical freezing in of structural disorder on cooling through a first-order thermodynamic liquid-solid transition without being able to rearrange so that the structure becomes stuck in a single of many thermodynamically equivalent disordered configurations. In two dimensions, where the liquid-to-crystal transition can be of infinite order with no discontinuity in entropy and no nucleation barrier to overcome,[1–3] the glass transition can be a thermodynamic transition in presence of disorder, shifting solidification to lower temperature.[4,5] Different disorder configurations might then be more accessible to exploration at temperatures below the glass transition. Our experiments, sensitive to disorder, support this view by showing that the disorder is still being dynamically sampled at all temperatures below the glass transition but that the sampling rate slows progressively as the temperature is reduced to give rise to metastability accompanied by field and temperature hysteresis strikingly similar to that found in 3D spin glasses.[6]

We investigate a 2D glass composed of supercurrent vortices. These constitute a very convenient system for studying the interaction and disorder problem: they are interacting objects which couple to disorder of the host material, their density is easily manipulated with the magnetic field and the interaction and persistence length can be varied by controlling the superconducting charge density. A quasi-two-dimensional system of vortices is created by applying a magnetic field perpendicularly to the strongly superconducting layers of a very anisotropic high-temperature superconductor, namely, $Bi_2Sr_2CaCu_2O_{8+\delta}$ (BSCCO). Because the coupling from plane to plane is weak, the vortex lines can easily lose continuity and spatially order themselves within each plane independently to form a collection of independent quasi-two-dimensional structures over a large temperature range. The disorder in the planes transforms what would have been 2D-ordered solids at low temperature into a decorrelated stack of 2D glassy solid structures of vortex segments ("pancake" vortices). The disorder in the vortex glass is observed by measuring the force required to depin it with a transport current.

Our host material BSCCO is a layered high-$T_c$ (critical temperature) superconductor with exceptionally low Josephson coupling between strongly superconducting planes. The high anisotropy carries over into the interaction between the in-layer vortices set up by a perpendicular magnetic field. The vortices interact logarithmically within the plane and both magnetically and by Josephson coupling between planes. While material inhomogeneity imposes the disorder, hole doping controls $T_c$, in-plane interaction and Josephson coupling strengths. Together with the wide range of thermal fluctuation afforded by the high $T_c$, these features allow access to a large variety of vortex structural phases. Experiments on optimally doped (for maximum $T_c$) material have shown that the vortices order in a classical 3D Abrikosov lattice at low fields, but quickly undergo a first-order transition (FOT) at higher fields into a stack of 2D glassy solids with evanescent correlation between layers. The field-temperature diagram of Fig. 1 shows the domains of existence of the various phases.[7–10]

The pinning of vortices in the 2D glass phase by host disorder is transmitted to the structure as a whole by virtue of the shear strength of the solid phase and this immobility of the totality of the vortices leads to vanishing dissipation (zero superconductor resistance). Above a temperature $T_{irr}(H)$, however, the magnetic moment has been found to become reversible,[11] signaling finite, though still nonlinear, vortex mobility. This is variously regarded as a 2D melting or glass transition.[12] This 2D glass phase displays a low-temperature region in which metastable configurations can exist, as revealed by irreversibility to field or temperature cycling.[13] The $(H,T)$ plane boundary line $T_p(H)$ of this region lies below the irreversibility line $T_{irr}(H)$ and coincides with a peak in the threshold current for finite resistivity when the sample has been prepared by setting the field at low temperature. This latter feature has so far not received any satisfactory explanation and is in the focus of the present

 

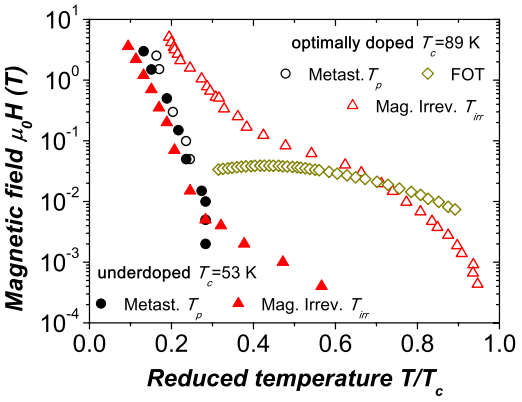


FIG. 1. (Color online) Principal boundaries for optimal and strongly underdoped BSCCO. The FOT for optimal doping was determined by local magnetic moment, Refs. 7 and 14, second magnetic hysteresis peak, Ref. 15, muon spin resonance, Ref. 10, neutron scattering (Ref. 8), and Josephson plasma resonance, Ref. 16. No FOT has been found for the present strong underdoping. $H_{irr}(T)$ corresponds to the onset of irreversibility of the magnetic moment, Ref. 11, signaling a glass phase. The metastability sets in below the peak $T_p(H)$ in ZFC threshold current, Ref. 13.

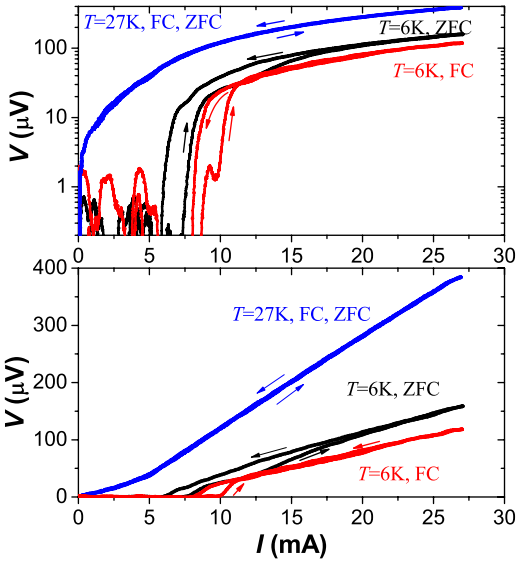


FIG. 2. (Color online) Experimental response of longitudinal potential drop vs superconductor transport current. The top and bottom frames refer to the same data which contribute to Fig. 3(a) while the arrows refer to increasing or decreasing current sweeps which occur in consecutive pairs.

work. Our experiments lead us to argue that the metastability results from a nonsingular slowing down in the dynamics of exploring different configurations to the time scale of the experiment, and not to a phase transition. We present a model which accounts well for the $T_p(H)$ dependence of the onset locus, for the characteristic features of the irreversible response to field and temperature and for the coincidence of the peak in threshold current with the onset of metastability.

## II. EXPERIMENT

We have complemented our previous experiments on optimally doped BSCCO (Ref. 13 and 17) with an additional set of experiments on strongly underdoped ($T_c \sim 50$ K) samples. The underdoped single crystals were grown by melt cooling and the doping was controlled by replacement of Ca by Pr. The chemical composition determined by secondary neutral mass spectrometry was $Bi_2Sr_2Ca_{0.87}Pr_{0.13}Cu_2O_{8+\delta}$ with critical temperatures as measured by zero-field resistance of 53 K and 51 K and transition widths of ~7 K. Electrical contacts were made by bonding gold wires with silver epoxy fired in $O_2$ at 900 K; the ~3 Ω current contacts enveloped the ends of the $\sim 1.2 \times 0.5 \times 0.005$ mm$^3$ samples and extended onto the two faces by ~100 μm. The ~70 μm dotlike potential contacts were placed symmetrically near the edges about 600 μm apart. The samples were mounted in the temperature-controlled bore of the same superconducting quantum interference device (SQUID) magnetometer which was used for the magnetic-moment measurements.

### A. Measurement

Two types of measurements were made: longitudinal voltage response to fast (10 μs duration to avoid sample heating[13]) triangular current pulses of up to 400 mA and contactless magnetic moment with a SQUID. Because the underdoped samples taken from two different batches fabricated one year apart gave similar results, we take them to be generic. The low-temperature $V$-$I$ characteristics show nonlinear prethreshold response terminating in a break in slope at a threshold current $I_{th}$.[17] The sensitivity to thermal and magnetic history in the metastable region led us to adopt a standard protocol: cool from $T > T_c$ at 4 K min$^{-1}$ to the preparation temperature, applying the field before cooling for field-cooled (FC) and after cooling for zero-field-cooled (ZFC). Measurements were made on warming unless stated. Three examples of $V$-$I$ response curves from which threshold currents are derived are given in Fig. 2.

The temperature dependence of the threshold currents at constant field for FC and ZFC always has the general features of Fig. 3. On warming, the low-temperature ZFC threshold increases to reach a maximum at temperature $T_p$, the same point at which the FC $I_{th}(T)$ shows an inflection or at most a broader, less marked maximum. Beyond $T_p$, both preparations show the same response with $I_{th}$ decreasing roughly as $T^{-2}$. Over the whole region $T < T_p(H)$ the $V$-$I$ characteristics reveal metastability; $V$-$I$ curves for FC become identical to those for ZFC if we impose a return field excursion up or down of $|\Delta H| \gtrsim 200$ Oe. Repeated current pulses also transform the FC $V$-$I$ toward the ZFC response, but never to fully attain it. The ZFC response, stable to field cycling, is irreversible in temperature. Figure 3(b) shows that the threshold current of a sample ZFC, prepared at low temperature $T_0 < T_p$ then heated at constant field to $T_1 < T_p$ and recooled, remains at the value it acquired at $T_1$. The same cycling phenomena are found for both optimal and underdoping, but only the underdoped samples show sensitivity to current pulses.

Figures 1 and 5 show how the metastability boundaries $T_p(H)$ for optimal and underdoped BSCCO map onto one

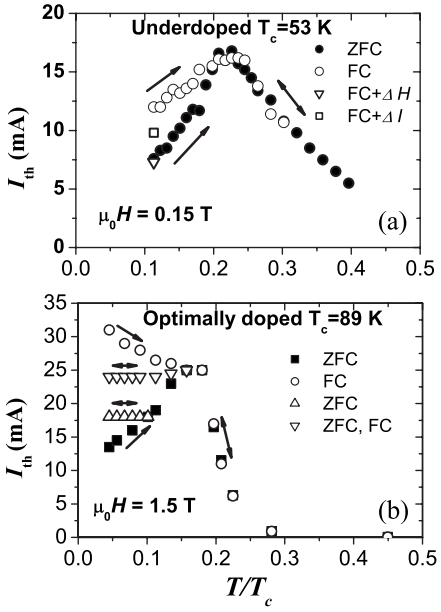


FIG. 3. Threshold current for FC and ZFC preparation at lowest temperature: (a) underdoped sample in $B=0.15$ T, showing instability to a return field excursion $\Delta B=\pm 200$ G and aging from a succession of current pulses $\Delta I$; (b) optimally doped sample where the effects of thermal cycling are also shown. Arrows indicate increasing or decreasing temperature.

another on scaling the temperature by $T_c$, with no scaling of the field, suggesting that the metastability does not depend on the crossover field for interplanar interaction[18,19] unlike the magnetic irreversibility lines. Furthermore, the relationship to the irreversibility line differs: the underdoped irreversibility merges with the metastability above about 4 mT, whereas the optimally doped irreversibility always lies well above the metastability, with any tendency to merge appearing only at the highest fields (>10 T). It is probable that we are always in the quasi-two-dimensional phase at low temperature for underdoping, for we found no second peak in the magnetic hysteresis which, for optimal doping at least, signals the 2D to 3D transition.

### B. Interpretation

Potential drop along a face arises from vortex motion across it, but the current density driving the vortices depends on how the interplane Josephson coupling modifies the current penetration, with the consequence that the *ab*-face threshold current becomes a combination of *ab* plane and *c*-axis thresholds.[20] For optimal doping the variation in the *ab*-face threshold current resembles that from bulk[21] and mesa[22,23] *c*-axis transport and Josephson plasma resonance,[16] leading us to suppose that it is dominated by the *c*-axis threshold. The resemblance to our underdoped *ab* face results suggests a similar situation: the threshold currents show principally the behavior of the *c*-axis Josephson critical current $J_J=J_J^0\langle\cos\phi_{n,n+1}\rangle$ between planes, $\phi_{n,n+1}$ being the superconductor phase difference between neighboring planes.[24] Lower disorder increases plane-to-plane correlation and enhances the critical current, implying that the ZFC state is more disordered than the FC. For given field and temperature, all values between FC and ZFC extremes can be attained, either by waiting[17] or by field or temperature cycling,[13] indicating a multiplicity of inequivalent, nonequilibrium disorder states.

## III. UNDERSTANDING

We must understand the form of the metastability onset line $T_p(H)$, its scaling between samples of different doping, the memory effects on temperature cycling and the astonishing sensitivity to field excursion. Any model must explain low-temperature metastability over times longer than the duration of the experiment, but admit sweeping through a large spread of different states on warming even though on recooling it remembers the turnaround state. This constraining set of features is contained in a simple model of Kramers escape kinetics in a strong pinning scenario which describes the structural dynamics as vortices trap and detrap on local disorder before losing contact with the thermal bath at low temperature. The sensitivity to sample preparation derives from compressive motion of the vortex network as the field is varied: for FC, the network is fixed whereas for ZFC the field variation sweeps the vortices over the traps enabling capture and consequently access to different disorder configurations not necessarily attained in thermal equilibrium.

### A. Model

Traps are supposed randomly distributed over the plane of the sample. The vortices constitute the vertexes of a regular elastic net, the cell size of which is determined by the magnetic field-vortex density relation and the elastic constants of which are set by the vortex-vortex interactions. The net is deformed by a vortex-trap interaction sufficiently sharp and deep that a vortex either remains centered on the undeformed net vertex or falls into a trap with concomitant elastic deformation of the net around it. The partition between trapped and untrapped vortices—or filled and empty traps—is determined by contact with a thermal reservoir which is modeled by Kramers escape rates. As the temperature is reduced there comes a "thermal disconnection" point below which thermal equilibrium cannot be established on the time scale of the experiment and metastability is observed in any phenomenon which is sensitive to the partition. In our experiment the phenomenon is the threshold current for dissipation which is determined by the disorder engendered by vortices attached to random traps. An important feature of this model is that as the field is varied the net shrinks or expands, thereby sweeping the vortices over the traps. Because the traps are randomly distributed, this appears in the reference of the net cell as random motion of traps moving in and out of the cell. For sufficient variation, any trap samples all positions in the cell.

Disorder is represented by strong, randomly positioned but dilute (many vortices per trap) traps with a distribution of trapping energies. We neglect interaction between trapping events. Traps are modeled by randomly distributed nonsuperconducting defects. The potential seen by a vortex at distance $\rho$ from a trap of radius $\eta$ is represented by an excluded

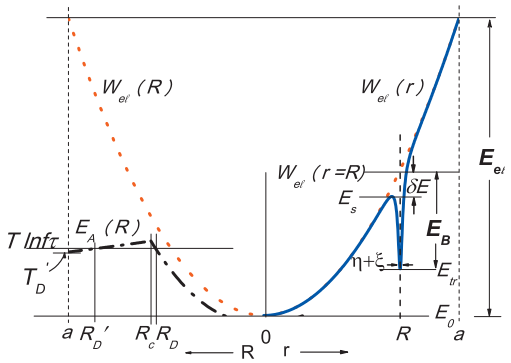


FIG. 4. (Color) Right side: sum of elastic and trapping potentials as a function of displacement $r$ of vortex from its lattice node. $a$ is the Wigner-Seitz radius, $R$ the position of the trap. Left side: the black dot-dash line shows the dominant activation energy $E_A$ of the Kramers escape processes as a function of trap position. Intersections of the horizontal line $T \ln f\tau$ with $E_A(R)$ delimit the metastable zone in the W-S cell.

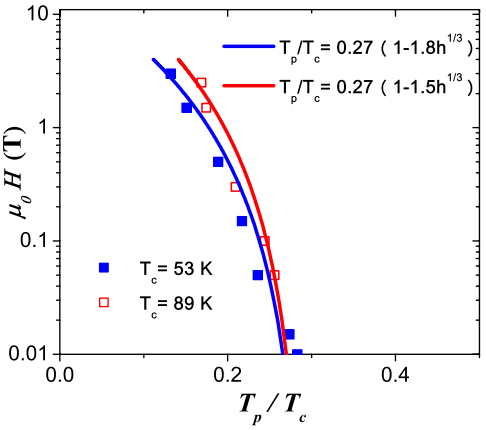


FIG. 5. (Color online) Experimental points and fit to Eq. (1) for the metastability boundary for optimal and underdoped samples.

volume potential $-W(\rho) \approx E_{kin}(\eta/\rho)^2$ truncated as $\rho \to \eta+\xi$ to $E_B \approx E_{kin} \ln \eta/\xi$ for $\eta > \xi$, the in-plane coherence length. $E_{kin}=(\Phi_0/4\pi\lambda_{ab})^2 s$, where $s$ is the interplane spacing, $\Phi_0$ is the flux quantum, and $\lambda_{ab}$ is the in-plane London screening length. It is the characteristic kinetic energy for a pancake vortex ($\sim$700 K for optimal doping). A trap at position **R** from the center of a Wigner-Seitz (W-S) cell of radius $a = \sqrt{B/\pi\Phi_0}$ preferentially captures the vortex of its own cell at an elastic strain energy cost of $W_{e\ell}(R)=E_{e\ell}(R/a)^2$, where $E_{e\ell} \propto E_{kin}$. The sum of these two energies has the asymmetric double-well structure of Fig. 4. As is easily appreciated from the figure, the thermal equilibrium trap occupancy $\langle p \rangle = 1 \ \forall \ R < R_c$ while $\langle p \rangle = 0 \ \forall \ R > R_c$, in the low-temperature limit $T \ll E_{e\ell}, E_B$, where $\exp|W_{e\ell} - E_B|/T \to \infty$, $R_c$ being the radius at which the energy of the two wells is equal: $W_{e\ell}(R_c)=E_B$.

### B. Metastability onset temperature

The thermal equilibration rate between wells[25] is determined by a sum of two processes: $\tau_{eq}^{-1}(T,R)=k_{\ell n \to tr}+k_{tr \to \ell n}$, where $k_{tr \to \ell n}=f_{tr} \exp -(E_s-E_{tr})/T$ is the Kramers escape rate from trap to lattice node and $k_{\ell n \to tr}=f_{\ell n} \exp -(E_s-E_0)/T$ is the inverse, $E_s$ being the energy at the saddle point between the two wells which lies along a radius toward the origin. The barrier to escape from the lattice node $E_s-E_0=W_{e\ell}(R) - \delta E$ and that for escape from the trap $E_s-E_{tr}=E_B-\delta E$, where $\delta E=3(E_{e\ell}^2 E_{kin})^{1/3}(R/a)^{2/3}(\eta/a)^{2/3}$ is calculated from the position of the saddle point of the potential. The relaxation rate is thus a function of the radial position $R$ of the trap in the W-S cell. Up to the crossover radius $R_c$, the first term dominates with activation energy $E_A=E_{e\ell}(R/a)^2-\delta E$ while beyond it the second term with activation $E_A=E_B - \delta E$ takes over with a steadily decreasing activation energy on approaching the cell edge, reflecting the lowering of the saddle point by the increasing slope of the elastic potential. The dominant activation energy is shown as the dot-dashed line on the left of Fig. 4. To re-establish equilibrium over the duration $\tau_{ex} \sim 10^2$ s of the experiment requires that $\tau_{eq}^{-1}(T,R) > \tau_{ex}^{-1}$, setting the temperature below which trap occupation can be metastable. On cooling, thermal contact is first lost for traps at $R=R_c$ which have the highest escape barrier; writing $\delta E/E_B$ in dimensionless form and $T_{p0} = E_B/\ln(f_{tr}+f_{\ell n})\tau_{ex}$, this onset temperature is given by

$$T_p(H) = T_{p0}(1 - \gamma h^{1/3}) \tag{1}$$

$h=H/H_{c2}$ and $\gamma=3(E_{e\ell}/E_{kin})^{1/3}(\eta/\sqrt{2}\xi \ln \eta/\xi)^{2/3} \sim 1$. We evaluate the escape rate prefactors by noting that the dynamical equations of vortices have the same form as massless electrons in a magnetic field. By transposing the results of Ref. 26 for the latter, we evaluate $f_{tr} \approx \hbar/2m^*(\xi^2+\eta^2) \sim 10^{12}$ s$^{-1}$ and $f_{\ell n}=(E_{e\ell}/E_{kin})\hbar/2m^*a^2=(E_{e\ell}/E_{kin})eB/4m^*c \sim 5\times 10^{10}$ s$^{-1}$ at $B=1$ T. Typically $\ln f\tau_{ex} \sim 30$.

Equation (1) is compared with the observed metastability onset line in Fig. 5, from which we find $T_{p0}=0.27T_c$ for both dopings while $\gamma \approx 1.8$ for optimal and $\gamma \approx 1.5$ for under doping. As regards scaling, $E_{e\ell} \propto E_{kin}$, the characteristic energy of $E_B$, is linear in $n_s/m^*$ ($m^*$ is the mass of the superconducting charges). $T_c$ is reported also to depend linearly on $n_s/m^*$,[27] suggesting that $T_{p0}$ should scale with $T_c$, at least to logarithmic accuracy in $\eta/\xi$, as it appears to do between our two samples of very different $T_c$. Using the estimates of escape rate prefactors, the experimental values for $T_{p0}$ yield $E_B \approx 770$ and 460 K for optimal and underdoped BSCCO, respectively, comparable to more direct, independent estimates for $E_{kin}$.

### C. Sensitivity to field variation

Varying the field compresses or expands the vortex lattice, slipping it with respect to the spatially fixed but randomly positioned traps. Viewed from the perspective of the traps, they find themselves moving through all positions in the W-S cell. When near the origin of the cell, they capture its vortex. To estimate the field increment necessary to allow any one trap to sample all positions in the cell, we note that an increment $\Delta H$ induces a vortex displacement **u** according to $n \nabla . \mathbf{u} \approx \delta n = \Delta H/\Phi_0$ and that in circular geometry $2u_r = r\delta n/n$. For disk radius $L$ and effective cross-section $\lesssim R_c < a$, the entire area of the disk is swept out by the network of

vortices when $\int au_r nrdr \gtrsim L^2$ or, in terms of field variation, $|\Delta H| \gtrsim \Delta H_{conv} \gtrsim 3\Phi_0/aL = 3\sqrt{\pi H \Phi_0/L^2}$. For a typical experiment at $\mu_0 H = 1$ T on a disk of radius $L = 0.2$ mm, a field variation in excess of only about $\Delta H_{conv} \gtrsim 10$ G could ensure that all traps have captured a vortex, maximizing the disorder because any filled trap in the metastable zone remains trapped. The variation required experimentally was about $10^2$ G.

### D. Nonequilibrium fraction at $T < T_p(H)$

Metastability exists when $T \ln f\tau < E_A$, the activation energy of the dominant Kramers rate, condition represented on the left of Fig. 4 by the horizontal line crossing $E_A(R)$. The intersections at $R_D$ and $R'_D$ delimit the metastable zone within the W-S cell and $T'_D$ is the temperature at which the outer equilibrium zone disappears. Metastability appears at the cusp point of the crossover of activation energies at $R = R_c$ as given by Eq. (1). At lower temperature, the cell is divided into two thermalized zones: $R < R_D$ with equilibrium trap occupancy $\langle p \rangle = 1$ and $R'_D < R < a$ with $\langle p \rangle = 0$. Trap occupancy of the middle, metastable, zone is preparation dependent. For FC preparation $\langle p \rangle = 1$ for $R < R_c$ and $\langle p \rangle = 0$ for $R > R_c$. Field variation $|\Delta H| > \Delta H_{conv}$ at fixed temperature $T_0$ establishes contact between it and the two equilibrium zones to give an intermediate value if $T'_D < T_0 < T_p$, but the outer zone vanishes when $T \le T'_D$ and the trap occupancy is then set by the inner region alone whence $\langle p \rangle = 1$ is transmitted to the entire cell area by traps transiting the inner capture zone.

The uniform spatial distribution of traps of fixed $E_B$ already leads to the spread $T_{p0}\gamma h^{1/3}\{(E_{e\ell}/E_B)^{1/3} - 1\}$ in thermal disconnection temperatures, seen for $R > R_c$ on the left of Fig. 4, and results in progressive growth of the metastable zone, but only over $T'_D < T_0 < T_p$. To account for the progressive behavior still observed at the lowest temperatures would require that $T'_D \to 0$ which in its turn demands an unreasonably extreme value of the ratio $E_{e\ell}/E_{kin} \gtrsim 6$ if the value of $T_{p0}$ is unique. However it is reasonable to expect a spread in $T_{p0} \propto E_B(\eta)$ accruing from a spread in $\eta$; this too extends the interval over which trap occupancy is progressively frozen in. A uniform distribution of $T_{p0}$ over the interval $[0, T_{\max}]$ would result, for ZFC preparation at $T_0 \le T$, in a concentration of occupied traps

$$c(T) \approx c_0 \left( \frac{T_{\max} - T}{T_{\max}} + \frac{T^2}{2T_{e\ell}T_{\max}} \right), \tag{2}$$

where $T_0 \le T < T_{\max}$, $T \ll E_B < E_{e\ell}$, $T_{e\ell} = E_{e\ell}/\ln f_{tr}\tau_{ex}$, and $c_0$ is the total trap concentration. Equation (2) is illustrated by the dotted line on Fig. 6. If the samples were ZFC prepared at zero temperature, all the traps would be occupied—occupancy 1 in the figure—and, upon heating, the zone over which the traps thermalize grows, emptying traps and decreasing the disorder to reach a minimum (floor) in trap occupancy at $T > T_{\max} = T_p$. Experimentally we observe a threshold current proportional to the Josephson $c$-axis threshold which is reduced by disorder. The sketch of the threshold current in Fig. 6 is what is to be expected if the reduction were to be linear in trap occupancy ($\partial I^c_{th}/\partial c < 0$). The measured threshold though depends on total disorder, so we must also add in the effect of vibrational fluctuations which transform what would have been a high-temperature $T > T_p$ plateau from the quasistatic disorder contribution, seen in the figure, into the decreasing function of temperature seen in experiment.

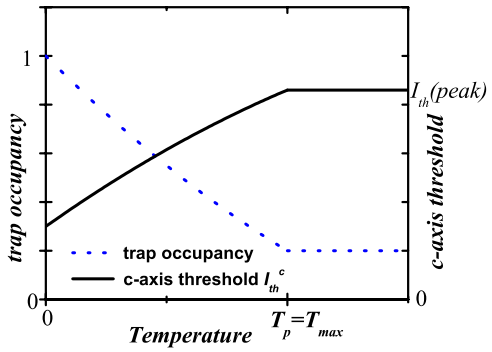


FIG. 6. (Color online) Prediction [Eq. (2)] of the model for trap occupancy on warming from a zero-field-cooled preparation. The $c$-axis threshold current curve is deduced from the trap occupancy supposing the two to be linearly related.

The thermal cycling experiments of Fig. 3 involve ZFC or field sweep preparation at temperature $T_0 < T_p$ followed by warming to $T_1 < T_p$ and recooling at constant field. On warming to $T_1 < T_p$, some traps empty by becoming thermally connected and have no reason to refill on recooling if the field is held constant, as indeed found experimentally [Fig. 3(b)].

## IV. CONCLUSION

Our experiments have shown that the 2D vortex glass phase in strongly underdoped BSCCO has the same generic behavior as for optimal doping. Both show metastability below a field-dependent temperature. There has been some doubt as to whether or not this metastability line betrays yet another phase transition. We conclude from the present study that it results from a dynamic crossover where thermal equilibrium between trapped and untrapped vortex sites is lost as the thermal relaxation becomes slower than the duration of the experiment. It does not, in itself, signal a phase transition, unless of course one chooses to define a glass transition by a freezing in of some disorder, but then one would have to accept that it occurs progressively over $T_p > T > 0$. To support our view we have shown that a simple model for the thermal relaxation dynamics, based on Kramers escape rates in an asymmetric double well, can account for all the features observed in the transport measurements: the functional dependence of the metastability onset temperature on field and its scaling with $T_c$, the differences between field-cooled and zero-field-cooled sample preparations, the extreme sensitivity to field variation with conversion from field-cooled to zero-field-cooled $V$-$I$ characteristics, the unusual increase in threshold current with temperature from a low-temperature zero field-cooled state as well as the coincidence of the peak in threshold current with the disappearance of metastability. These slow relaxation fluctuations are superimposed on the fast vibrational disorder. Although the onset of metastability

does not in itself mark a phase transition, activated slowdown can only set in once the glassy solid phase is attained so that the metastability and magnetic irreversibility lines can, but do not necessarily, merge. The essential hypothesis is a disordered multiwell situation in configuration space, but as that is not unique to strong pinning, the success of our model is not a definitive proof of this type of pinning, but the reasonableness of the parameters required to fit experiment does give it some credence.

Clearly this 2D glass is not stuck irremediably in a sole disorder configuration as in 3D glasses. Nonetheless, the remarkable likeness to the preparation history properties of the 3D spin-glass susceptibility, both in observation[6] and in modeling,[28,29] points to more similarity between the two systems than one might have expected.

## ACKNOWLEDGMENTS

We have benefitted from stimulating discussion with Titusz Feher and Istvan Tutto and we are grateful to the Hungarian OTKA funding agency under Grant No. K 62866. The research in Lausanne was supported by the pool "MaNEP" of the Swiss NSF.

[1] D. R. Nelson and B. I. Halperin, Phys. Rev. B **19**, 2457 (1979).
[2] J. Kosterlitz and D. Thouless, J. Phys. C **6**, 1181 (1973).
[3] D. Nelson, *Defects and Geometry in Condensed Matter Physics* (Cambridge University Press, 2002), Chap. 3.
[4] D. R. Nelson, Phys. Rev. B **27**, 2902 (1983).
[5] M.-C. Cha and H. A. Fertig, Phys. Rev. Lett. **74**, 4867 (1995).
[6] G. G. Kenning, D. Chu, and R. Orbach, Phys. Rev. Lett. **66**, 2923 (1991).
[7] E. Zeldov, D. Majer, M. Konczykowski, V. Geshkenbein, V. Vinokur, and H. Shtrikman, Nature (London) **375**, 373 (1995).
[8] R. Cubitt *et al.*, Nature (London) **365**, 407 (1993).
[9] M. B. Gaifullin, Y. Matsuda, N. Chikumoto, J. Shimoyama, and K. Kishio, Phys. Rev. Lett. **84**, 2945 (2000).
[10] C. Bernhard *et al.*, Phys. Rev. B **52**, R7050 (1995).
[11] A. Schilling, R. Jin, J. D. Guo, and H. R. Ott, Phys. Rev. Lett. **71**, 1899 (1993).
[12] H. Safar, P. L. Gammel, D. J. Bishop, D. B. Mitzi, and A. Kapitulnik, Phys. Rev. Lett. **68**, 2672 (1992).
[13] B. Sas, F. Portier, K. Vad, B. Keszei, L. F. Kiss, N. Hegman, I. Puha, S. Mészáros, and F. I. B. Williams, Phys. Rev. B **61**, 9118 (2000).
[14] H. Beidenkopf, N. Avraham, Y. Myasoedov, H. Shtrikman, E. Zeldov, B. Rosenstein, E. H. Brandt, and T. Tamegai, Phys. Rev. Lett. **95**, 257004 (2005).
[15] Y. Yeshurun, N. Bontemps, L. Burlachkov, and A. Kapitulnik, Phys. Rev. B **49**, 1548 (1994).
[16] Y. Matsuda, M. B. Gaifullin, K.-i. Kumagai, M. Kosugi, and K. Hirata, Phys. Rev. Lett. **78**, 1972 (1997).
[17] F. Portier, G. Kriza, B. Sas, L. F. Kiss, I. Pethes, K. Vad, B. Keszei, and F. I. B. Williams, Phys. Rev. B **66**, 140511(R) (2002).
[18] M. Feigel'man, V. Geshkenbein, and A. Larkin, Physica C **167**, 177 (1990).
[19] L. I. Glazman and A. E. Koshelev, Phys. Rev. B **43**, 2835 (1991).
[20] I. Pethes, A. Pomar, B. Sas, G. Kriza, K. Vad, A. Pallinger, F. Portier, and F. I. B. Williams, Phys. Rev. B **68**, 184509 (2003).
[21] F. de la Cruz, E. Rodriguez, H. Pastoriza, A. Arribére, and M. F. Goffman, Physica B **197**, 596 (1994).
[22] A. Yurgens, D. Winkler, T. Claeson, G. Yang, I. F. G. Parker, and C. E. Gough, Phys. Rev. B **59**, 7196 (1999).
[23] M. Suzuki, T. Watanabe, and A. Matsuda, Phys. Rev. Lett. **81**, 4248 (1998).
[24] L. N. Bulaevskii, M. P. Maley, and M. Tachiki, Phys. Rev. Lett. **74**, 801 (1995).
[25] P. Hänggi, P. Talkner, and M. Borkovec, Rev. Mod. Phys. **62**, 251 (1990).
[26] R. Filliger and P. Reimann, Europhys. Lett. **77**, 30008 (2007).
[27] Y. J. Uemura *et al.*, Phys. Rev. Lett. **62**, 2317 (1989).
[28] D. Walton, Phys. Rev. Lett. **100**, 027207 (2008).
[29] S.-k. Ma, Phys. Rev. B **22**, 4484 (1980).